



## Climate Change and Agriculture Research Paper

**Cite this article:** Wang X *et al.* (2024). Comparison of four upscaling methods to drive instantaneous evapotranspiration to daily values for maize in two climatic regions in China. *The Journal of Agricultural Science* 1–14. <https://doi.org/10.1017/S0021859624000637>

Received: 21 June 2024  
Revised: 18 September 2024  
Accepted: 22 September 2024

### Keywords:

crop coefficient method; direct canopy resistance method; evaporative fraction method

### Corresponding author:

Haofang Yan;  
Email: [yanhaofangyh@163.com](mailto:yanhaofangyh@163.com)

# Comparison of four upscaling methods to drive instantaneous evapotranspiration to daily values for maize in two climatic regions in China

Xuanxuan Wang<sup>1</sup> , Biyu Wang<sup>1</sup> , Haofang Yan<sup>1,3</sup>, Chuan Zhang<sup>2</sup>, Hexiang Zheng<sup>4</sup>, Guoqing Wang<sup>3</sup>, Jianyun Zhang<sup>3</sup>, Rongxuan Bao<sup>1</sup>, Run Xue<sup>2</sup>, Yudong Zhou<sup>1</sup>, Jun Li<sup>2</sup>, Rui Zhou<sup>1</sup>, Bin He<sup>5</sup>, Beibei Hao<sup>5</sup> and Yujing Han<sup>1,5</sup>

<sup>1</sup>Research Centre of Fluid Machinery Engineering and Technology, Jiangsu University, Zhenjiang 212013, China; <sup>2</sup>School of Agricultural Equipment Engineering, Jiangsu University, Zhenjiang 212013, China; <sup>3</sup>State Key Laboratory of Hydrology-Water Resources and Hydraulic Engineering, Nanjing Hydraulic Research Institute, Nanjing 210029, China; <sup>4</sup>Institute of Pastoral Hydraulic Research, China Institute of Water Resources and Hydropower Research, Hohhot 010020, China and <sup>5</sup>National-Regional Joint Engineering Research Center for Soil Pollution Control and Remediation in South China, Guangdong Key Laboratory of Integrated Agro-environmental Pollution Control and Management, Institute of Eco-environmental and Soil Sciences, Guangdong Academy of Sciences, Guangzhou 510650, China

### Abstract

Accurately converting satellite instantaneous evapotranspiration ( $\lambda ET_i$ ) over time to daily evapotranspiration ( $\lambda ET_d$ ) is crucial for estimating regional evapotranspiration from remote sensing satellites, which plays an important role in effective water resource management. In this study, four upscaling methods based on the principle of energy balance, including the evaporative fraction method (*Eva-f* method), revised evaporative fraction method (*R-Eva-f* method), crop coefficient method ( $K_c$ - $ET_0$  method) and direct canopy resistance method (*Direct- $r_c$*  method), were validated based on the measured data of the Bowen ratio energy balance system (*BREB*) in maize fields in northwestern (NW) and northeastern (NE) China (semi-arid and semi-humid continental climate regions) from 2021 to 2023. Results indicated that *Eva-f* and *R-Eva-f* methods were superior to  $K_c$ - $ET_0$  and *Direct- $r_c$*  methods in both climatic regions and performed better between 10:00 and 11:00, with mean absolute errors (*MAE*) and coefficient of efficiency ( $\epsilon$ ) reaching  $<10 \text{ W/m}^2$  and  $> 0.91$ , respectively. Comprehensive evaluation of the optimal upscaling time using global performance indicators (*GPI*) showed that the *Eva-f* method had the highest *GPI* of 0.59 at 12:00 for the NW, while the *R-Eva-f* method had the highest *GPI* of 1.18 at 11:00 for the NE. As a result, the *Eva-f* approach is recommended as the best way for upscaling evapotranspiration in NW, with 12:00 being the ideal upscaling time. The *R-Eva-f* method is the optimum upscaling method for the Northeast area, with an ideal upscaling time of 11:00. The comprehensive results of this study could be useful for converting  $\lambda ET_i$  to  $\lambda ET_d$ .

## Introduction

Understanding the regional water consumption and distribution plays an essential role in indicating crop water consumption and determining irrigation strategies (Ma *et al.*, 2021; Disasa *et al.*, 2024). Evapotranspiration (*ET*), equivalent form of the latent heat flux ( $\lambda ET$ ), contributes significantly to the energy balance of farmed surfaces (Gao *et al.*, 2018; Yan *et al.*, 2018; Wang *et al.*, 2024b), and is a key consideration for addressing a number of scientific and engineering issues, such as the hydrological cycles, climate change and carbon cycle (Ma *et al.*, 2019; Xu *et al.*, 2020; Liu *et al.*, 2022; Lakhari *et al.*, 2024).

Farmland *ET* is estimated by several methods such as water balance (Choudhury *et al.*, 2013; Jiang *et al.*, 2014), lysimeters (Evetts *et al.*, 2012) and micrometeorological methods such as eddy covariance (Hossen *et al.*, 2011; Yang *et al.*, 2016) and Bowen ratio energy balance (Zhang *et al.*, 2010; Pozníková *et al.*, 2018; Yan *et al.*, 2023; Li *et al.*, 2024). However, the limitations of typical observation approaches include poor spatial representation, expensive installations, and only providing point measurements (Liu *et al.*, 2012b).

In recent decades, remote sensing *ET* retrieval based on the combination of satellite remote sensing data and the land surface energy model has become an increasingly important area of research, as it can provide spatial distributions of surface information, solve the problem of bad spatial representativeness of the methods for point scale, and provide an effective way of calculating *ET* (Jung *et al.*, 2010; Miralles *et al.*, 2011; Mu *et al.*, 2011; Zhang *et al.*, 2019).

Nevertheless, remotely sensed data-based *ET* estimate algorithms can only compute an instantaneous energy budget at the time of the satellite overpass, which is not able to meet the requirements of *ET* on daily as well as longer time scale in practical applications (Delogu et al., 2012; Liu et al., 2017). Accurate daily *ET* can provide important guidance for water resources management, hydrological cycle studies and establishment of rational irrigation schedules (Tang et al., 2013). It is, therefore, necessary to develop temporal upscaling methods in order to upgrade *ET* from an instantaneous to a daily scale (Jiang et al., 2021), which may be an effective way to address the problem that remote sensing only provides a basic instantaneous estimate of *ET*, and this scaling-up relationship should be investigated and demonstrated through studies that primarily use localized (*in situ*) observations. In addition, the applicability of the upscaling approach to different ecosystems should be assessed, especially in water resources studies (Van Niel et al., 2012).

Most of the existing upscaling methods in practice are developed based on daily stability or regularity properties in instantaneous *ET* estimation models (Chávez et al., 2008; Cammalleri et al., 2014). Relating daily *ET* ( $\lambda ET_d$ ) to a component that can be almost constant during the day or throughout a diurnal cycle is crucial to the development of different upscaling methods (Farah et al., 2004; Liu et al., 2012a). The factor can be stated as the ratio of an hourly computable reference variable to instantaneous *ET* ( $\lambda ET_i$ ) at a given time of day (Van Niel et al., 2012; Tang et al., 2013; Cammalleri et al., 2014). Several methods, including the evapotranspiration fraction method, the crop coefficient method, the canopy resistance method, the Katerji Perrier method, the advective drought method, and the daily sinusoidal function, can be used to estimate  $\lambda ET_d$  based on the assumption that the diurnal course of *ET* is similar to that of the solar irradiance.

The evaporative fraction ( $E_f$ ), defined as the ratio between latent heat flux and available energy at the surface, is an important parameter that reflects the distribution of available energy at the surface and explains the components of the energy budget (Shuttleworth et al., 1989). Many studies have been conducted to test the validity of the evaporative fraction method (*Eva-f* method) utilizing local available energy observations and the self-preservation assumption that  $E_f$  remains roughly constant throughout the day. Tang et al. (2013) and Zhang et al. (2017) found that the *Eva-f* method accurately estimates  $\lambda ET_d$  for winter wheat and summer maize in Northern China and semiarid northwest China, respectively. However, previous studies have revealed that a range of environmental factors has an impact on the assumption of self-preservation (Farah et al., 2004; Gentine et al., 2007; Xu et al., 2015; Wandera et al., 2017). The  $E_f$  during the daytime is largely time related and depends strongly on soil moisture effectiveness, canopy cover, developmental stage, relative humidity, and the biological characteristics of vegetation in an area (Gentine et al., 2007; Hoedjes et al., 2008), while the surface energy budget affects the microclimate of the vegetation canopy (Hossen et al., 2011). These variable environmental factors may lead to inaccuracies in  $\lambda ET_d$  estimates when using the *Eva-f* method. As a result, there is no consensus on the overall trend of daytime  $E_f$  fluctuations, which may vary from site to site (Van Niel et al., 2011). Tang et al. (2013) and Van Niel et al. (2012) implied that the  $E_f$  is more variable under cloudy conditions compared to clear sky conditions. The daily shape of  $E_f$  depends on atmospheric forcing and surface conditions (Gentine et al., 2007); the  $E_f$  typically remains constant in the

morning and increases sharply in the afternoon (Gentine et al., 2007; Delogu et al., 2012). Gentine et al. (2007) and Hoedjes et al. (2008) found that the  $E_f$  fluctuates more in humid areas, whereas the *Eva-f* method performs best in arid areas. In addition, the  $E_f$  was also affected by effective energy, which varied little in areas with high effective energy during the day (Li et al., 2008). When the leaf area index is large, the  $E_f$  is less stable for the same amount of soil moisture (Gentine et al., 2007). Allen et al. (2007) noted a consistent decrease in hourly  $E_f$  for mowed grass, whereas sugarbeet had a significant increase in  $E_f$  in the afternoon. Chemin and Alexandridis (2001) suggested that assuming soil heat flux ( $G$ ) equal to 0 may significantly improve the accuracy of the *Eva-f* method for calculating  $\lambda ET_d$  because the  $G$  is a low percentage of the surface energy balance and always varies with soil thermal properties and soil moisture. Therefore, a revised evaporative fraction method (*R-Eva-f* method) was developed to calculate the  $\lambda ET_d$  using a modified evaporative fraction ( $RE_f$ ), which is the proportion of  $\lambda ET$  to net radiation ( $R_n$ ). Suleiman and Crago (2004) found that the *R-Eva-f* method is more effective for extrapolating  $\lambda ET_d$  from time-by-time measurements in grasslands. Chávez et al. (2008) showed that the *R-Eva-f* method overestimates  $\lambda ET_d$  in maize and soybean fields.

Allen et al. (2007) found that the crop coefficient ( $K_c$ ), which is the ratio of *ET* to reference evapotranspiration ( $ET_0$ ), is almost constant at low daylight frequencies, which applied to *ET* magnification and was named the crop coefficient method ( $K_c-ET_0$  method). Several experiments have successfully estimated the  $\lambda ET_d$  from instantaneous values using the  $K_c-ET_0$  method, which considers the influence of atmospheric characteristics (Delogu et al., 2012; Xu et al., 2015; Zhang et al., 2017). The  $K_c-ET_0$  method performed well over agricultural irrigated areas (Allen et al., 2007), but poorly over bare soil where *ET* decreased rapidly (Colaizzi et al., 2006).

Furthermore, the direct canopy resistance method (*Direct- $r_c$*  method) was developed by Farah et al. (2004) to estimate the  $\lambda ET_d$  from the  $\lambda ET_i$  based on a diurnal fluctuation of canopy resistance ( $r_c$ ). The effectiveness of the *Direct- $r_c$*  method has been validated by numerous studies (Tang et al., 2017; Zhang et al., 2017; Yan et al., 2022b). Tang et al. (2017) and Yan et al. (2022b) reported that the *Direct- $r_c$*  method did not yield a much closer scaled  $\lambda ET_d$  when utilizing varied  $r_c$  as opposed to fixed  $r_c$ . They also noted that the assumption that the  $r_c$  would be virtually constant during the day was dubious and that more research was necessary.

A number of comparative analyses have also been carried out to evaluate the precision and suitability of various upscaling methods. As for the comparison of the *ET* scaling up methods based on  $E_f$ ,  $K_c$  and  $r_c$ , Colaizzi et al. (2006) and Xu et al. (2015) showed that the estimated  $\lambda ET_d$  based on the *Eva-f* method fitted measured values better for non-vegetated land cover, while the  $K_c-ET_0$  method and *Direct- $r_c$*  method had the best performance during the season of vegetation growth. Chávez et al. (2008) found that the  $K_c-ET_0$  method performed better under uniform vegetation cover, whereas the *R-Eva-f* method overestimates  $\lambda ET_d$  for both corn and soybean fields. Yan et al. (2022b) noted that in circumstances where there is a significant departure from reference grass, the  $K_c-ET_0$  method may not perform well. Tang et al. (2013) used eddy-correlation data from northern China to assess the efficacy of four upscaling methods, and showed that the  $K_c-ET_0$  method was the most accurate in the clear and partly cloudy skies. Another comparative study based on four upscaled methods was also conducted in Australia, and

the *Direct- $r_c$*  method was used to calculate  $\lambda ET_d$  for maize and canola crops, with a high degree of consistency with eddy-correlation systems (Liu *et al.*, 2012a). Zhang *et al.* (2017) found that the *Eva-f* and *K<sub>c</sub>-ET<sub>0</sub>* methods gave the best performance when using instantaneous values from 11:00 to 15:00. Yan *et al.* (2022b) reported that the *Eva-f* and *R-Eva-f* methods gave the best performance when using instantaneous values for the time period 11:00–14:00.

Previous studies have shown that the accuracy and applicability of different upscaling methods are affected by factors such as ecosystem, location, instantaneous time of upscaling and meteorological data. The performance of the above upscaling methods at instantaneous time may be different under different satellite traversal times, climatic conditions and vegetation growth conditions. Thus, the objectives of this study were (1) to evaluate the performances of the four scaling methods (*Eva-f*, *R-Eva-f*, *K<sub>c</sub>-ET<sub>0</sub>* and *Direct- $r_c$*  method) in estimation of the  $\lambda ET_d$  from  $\lambda ET_i$  for maize grown in two climatic regions (semi-arid and semi-humid continental climate); (2) to comprehensively evaluate the optimal scale-up times of the four models by adopting global performance indicators (GPI); (3) to analyse the differences of these methods under two climatic regions and (4) to recommend proper approaches for estimating  $\lambda ET_d$  and the optimal upscaling time for two climatic regions.

## Materials and methods

### Field observations

The experimental data used in this study were obtained from two long-term automatic meteorological stations in northwestern and

northeastern China. The experiment in northwestern China (NW) was conducted in a maize field located at Ordos city (39° 53' N, 109°60' E, 1456 m a.s.l.) from May 2022 to September 2023. It is a semi-arid temperate continental monsoon area with abundant sunshine resources, average hours of sunshine are more than 3000 h per year, the average annual temperature is 12.9 °C, the average annual precipitation ranges from 190 to 300 mm, the evaporation of free water surface is 1500 mm and the frost-free period is 150 days. The soil texture is primarily sandy soil, with an average soil bulk density and field water-holding capacity of 1.60 g/cm<sup>3</sup> and 24.7%, respectively. The experiment in northeastern China (NE) was conducted in a maize field located at Harbin city (45°38' N, 126°22' E, 140 m a.s.l.) from May 2021 to October 2022. It has a temperate semi-moist continental monsoon climate, with rainfall mainly occurring from June to September, and the average annual precipitation ranges from 500 to 600 mm. The average annual temperature is about 6.9°C, with the highest and lowest average monthly temperatures occurring in July (23.7°C) and January (−13.5°C), respectively. The soil texture is primarily loamy, with an average bulk density and field water-holding capacity of 1.35 g/cm<sup>3</sup> and 32.0%, respectively. The location and precipitation information for both sites are shown in Fig. 1. The precipitation data were obtained from the Geographic Data Sharing Infrastructure (GDSI), Global Resource Data Cloud ([www.gis5g.com](http://www.gis5g.com)).

Two sets of Bowen ratio energy balance (*BREB*) observation systems were installed in the centre of the maize fields at the NW and NE China experimental stations (Yan *et al.*, 2022b). The study fields were surrounded by other similar crops and the installation heights of the probes used to observe the

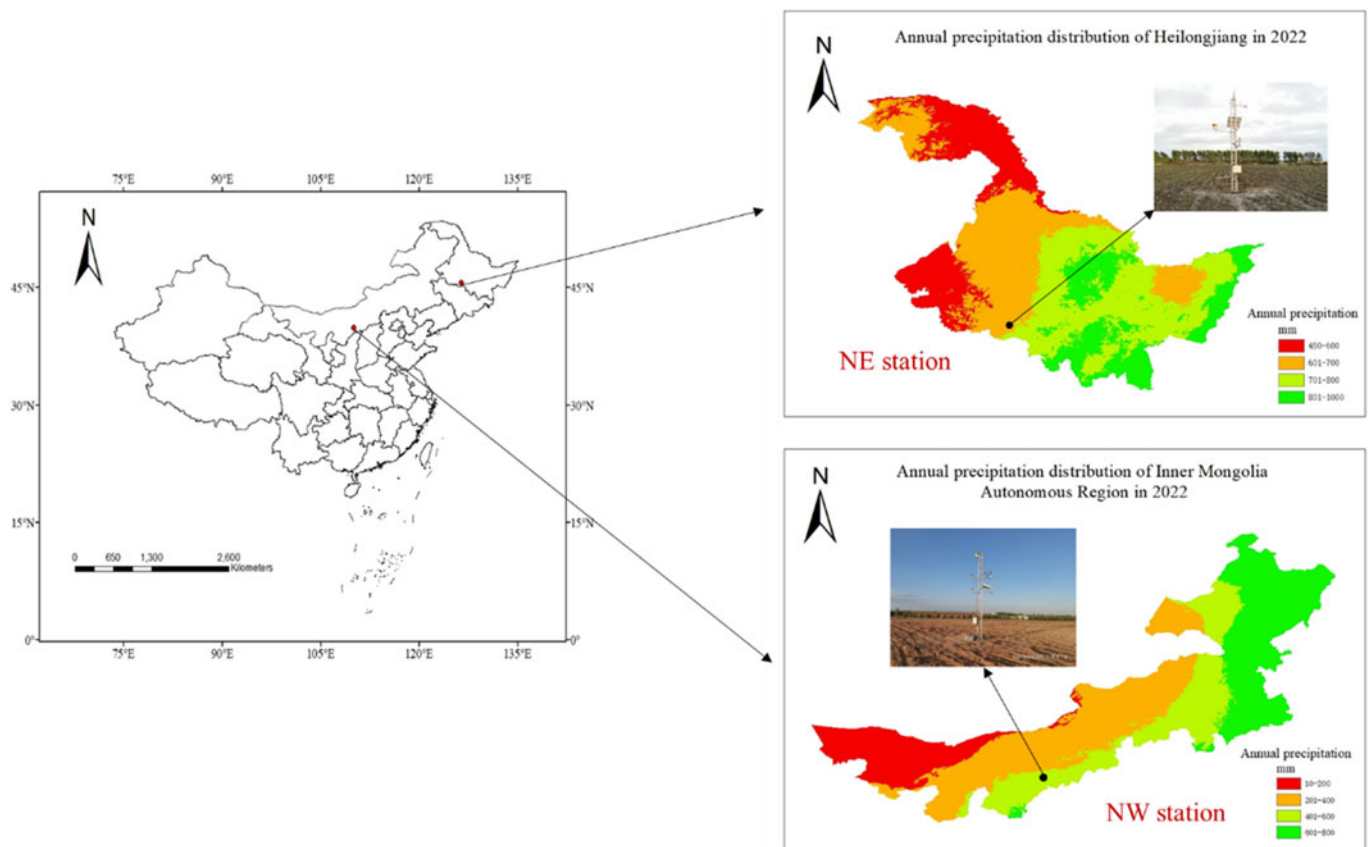


Figure 1. Locations of the two climatic regions of northern China.

temperature and humidity were low (50–100 cm above the canopy), so adequate fetch length (> 100–200 m) can be provided (Yan *et al.*, 2021). Net radiation ( $R_n$ ) of maize fields at two sites was measured by CNR-4 sensors (Kipp and Zonen, Netherlands) at 4 m for NW and 3 m for NE above the ground; wind speed ( $u$ ) was measured by three-cup anemometers, A100L2 (MetOne, USA, with an accuracy of  $\pm 0.12$  m/s), at 6 m for NW and 4 m for NE above the ground; and the air temperature ( $T_a$ ) and relative humidity ( $RH$ ) were measured with HMP155A sensors (Vaisala, Finland, accuracy  $\pm 0.1^\circ\text{C}$  for  $T_a$  and  $\pm 2\%$  for  $RH$ ) at 3 and 4 m above the ground for NW station, and at 3.5 and 4.5 m above the ground for NE station for the Bowen ratio energy balance (*BREB*) method; the volumetric soil water content (*VWC*) was measured by five TDR-315H sensors (Acclima, USA) at depths of 20, 40, 60, 80 and 100 cm at the centre of the field at NW station; four TDR-315H sensors (Acclima, USA) were used in NE station to measure the *VWC* at 5, 10, 20 and 100 cm; the soil heat flux ( $G$ ) measurements in both stations were carried out using soil heat flux panels HFP01-L10 (Campbell Scientific, USA) and rainfall ( $P$ ) was measured using TE525MM (Campbell Scientific, USA). All sensors were connected to a CR1000 data logger (Campbell Scientific, USA), with an average sampling frequency of every 10 min (Jiang *et al.*, 2024). The accuracy of all sensors was verified prior to installation. Data are missing from 12 May 2022 to 29 May 2022 at the NW station and from 21 August 2022 to 14 September 2022 at the NE station due to instrument failure. The date format used was ISO 8601 time format ([https://en.wikipedia.org/wiki/ISO\\_8601](https://en.wikipedia.org/wiki/ISO_8601)).

### Scaling up methods

#### *Eva-f* method

The evaporative fraction (*Eva-f*) method can be expressed as (Sugita and Brutsaert, 1991):

$$E_f = \frac{\lambda ET_i}{(R_n - G)_i} \quad (1)$$

$$\lambda ET_d = E_f(R_n - G)_d \quad (2)$$

where  $E_f$  is the evaporative fraction at a certain hourly time,  $\lambda ET_i$  and  $\lambda ET_d$  are the latent heat flux at time  $i$  and total daytime, respectively ( $\text{W/m}^2$ ).  $R_n$  and  $G$  are the net radiation and soil heat flux ( $\text{W/m}^2$ ) and  $\lambda$  is the latent heat of vaporization ( $\text{J/kg}$ ). The subscripts  $i$  and  $d$  express the instantaneous time of day and total daytime values, respectively.

#### *R-Eva-f* method

The revised evaporative fraction (*R-Eva-f*) method estimating  $\lambda ET_d$  from  $\lambda ET_i$  was proposed on the assumption that the daily mean value of the soil heat flux ( $G$ ) in *Eva-f* method is zero (Chemin and Alexandridis, 2001) and expressed as follows:

$$RE_f = \frac{\lambda ET_i}{R_{ni}} \quad (3)$$

$$\lambda ET_d = RE_f \times R_{nd} \quad (4)$$

where  $RE_f$  is the ratio of  $\lambda ET_i$  and  $R_{ni}$  at a certain hourly time, other symbols have the same meanings as in (Eqns (1) and (2)).

#### *K<sub>c</sub>-ET<sub>0</sub>* method

The crop coefficient (*K<sub>c</sub>-ET<sub>0</sub>*) method to estimate  $\lambda ET_d$  from  $\lambda ET_i$  based on the crop coefficient ( $K_c$ ) can be expressed as follows (Colaizzi *et al.*, 2006):

$$\lambda ET_{0i} = \frac{\Delta_i(R_n - G)_i + \rho_a C_p VPD_i u_{2i} / 208}{\Delta_i + \gamma_i(1 + 0.34u_{2i})} \quad (5)$$

$$K_{ci} = \frac{\lambda ET_i}{\lambda ET_{0i}} \quad (6)$$

$$\lambda ET_d = K_{ci} \times \lambda ET_{0d} \quad (7)$$

where  $K_c$  is the crop coefficient at a certain hourly time,  $\lambda ET_0$  is the latent heat flux from the reference crops ( $\text{W/m}^2$ ),  $\Delta$  is the slope of the saturation vapour pressure curve ( $\text{kPa}/^\circ\text{C}$ ),  $\rho_a$  is the air density ( $\text{kg/m}^3$ ),  $C_p$  is the specific heat of dry air at constant pressure ( $\text{J/kg/K}$ ),  $VPD$  is the vapour pressure deficit ( $\text{kPa}$ ),  $\gamma$  is the psychrometric constant ( $\text{kPa}/^\circ\text{C}$ ), and  $u_2$  is the wind speed at 2 m height (m/s), the subscripts  $i$  and  $d$  express the instantaneous time of day and total daytime values, respectively.

#### *Direct-r<sub>c</sub>* method

The direct canopy resistance (*Direct-r<sub>c</sub>*) method to estimate  $\lambda ET_d$  from  $\lambda ET_i$  based on  $r_c$  can be expressed as follows (Malek *et al.*, 1992):

$$r_c = r_{ai} \times \left[ \left( \frac{\Delta_i(R_n - G)_i + \frac{\rho_a C_p VPD_i}{r_{ai}}}{\lambda ET_i} - \Delta_i \right) \frac{1}{\gamma_i} - 1 \right] \quad (8)$$

$$\lambda ET_d = \frac{\Delta_d(R_n - G)_d + \frac{\rho_a C_p VPD_d}{r_{ad}}}{\Delta_d + \gamma_d \left( 1 + \frac{r_c}{r_{ad}} \right)} \quad (9)$$

where  $r_a$  is the aerodynamic resistance (s/m),  $r_c$  is the canopy resistance (s/m), the subscripts  $i$  and  $d$  express the instantaneous time of day and total daytime values, respectively.

The value of  $r_a$  was calculated by (Thom, 1972):

$$r_a = \frac{\ln \frac{z-d}{z_0} \ln \frac{z-d}{z_{0h}}}{\kappa^2 u_z} \quad (10)$$

where  $z$  is the height of wind measurements (m),  $d$  is the zero plane displacement height (m) estimated as  $d = 0.67h_c$ ,  $h_c$  is the mean height of the crop (m),  $z_0$  is the roughness length governing momentum transfer (m) calculated as  $z_0 = 0.123h_c$ ,  $z_{0h}$  is the roughness length governing transfer of heat and vapour (m) computed as  $z_{0h} = 0.1z_0$ ,  $u_z$  is the wind speed at height  $z$  (m/s), and  $\kappa$  is the von Karman constant ( $= 0.41$ ).



Evapotranspiration measurements

One of the standard techniques for measuring  $\lambda ET$  indirectly is the Bowen ratio energy balance (*BREB*) method (Pozníková *et al.*, 2018; Yan *et al.*, 2022a). The *BREB* determines the latent heat and sensible heat fluxes based on the rearrangement of the simplified surface energy balance equation given by (Heilman and Brittin, 1989):

$$\lambda ET_i = \frac{R_n - G}{1 + \beta} \tag{11}$$

$$\beta = \frac{H}{\lambda ET_i} = \gamma \frac{\Delta T}{\Delta e} \tag{12}$$

where  $\beta$  is the Bowen ratio,  $\Delta T$  is the air temperature gradient and  $\Delta e$  is the actual vapour pressure gradient. The measured  $\lambda ET_d$  were computed by the sum of  $\lambda ET_i$  which was obtained using the *BREB* method based on the hourly meteorological data from 8:00 to 16:00 for both areas. To control the measurement quality, the  $\lambda ET$  results were ignored when  $\beta$  was close to  $-0.75$  (Ohmura, 1982).

Performance evaluation

The relative performance of the four upscaling methods was evaluated using the statistical indices, including coefficient of determination ( $R^2$ ), mean absolute error (*MAE*), relative root mean absolute error (*RRMSE*) and coefficient of efficiency ( $\epsilon$ ).

$$MAE = \frac{1}{n} \sum_{i=1}^n |E_i - O_i| \tag{13}$$

$$RRMSE = \frac{\sqrt{\frac{1}{n} \sum_{i=1}^n (E_i - O_i)^2}}{\bar{O}} \tag{14}$$

$$\epsilon = 1.0 - \frac{\sum_{i=1}^N |O_i - E_i|}{\sum_{i=1}^N |O_i - \bar{O}|} \tag{15}$$

where  $E_i$  and  $O_i$  represent the estimated and observed values, respectively,  $n$  is the total sample number and  $\bar{O}$  is the mean of observed values.  $R^2$  represents the degree of replication of the model to the observed value. The higher the value of  $R^2$  is, the better the performance is. Both *RRMSE* and *MAE* values are range from 0 (perfect fit) to  $\infty$  (worst fit).  $\epsilon$  is dimensionless,

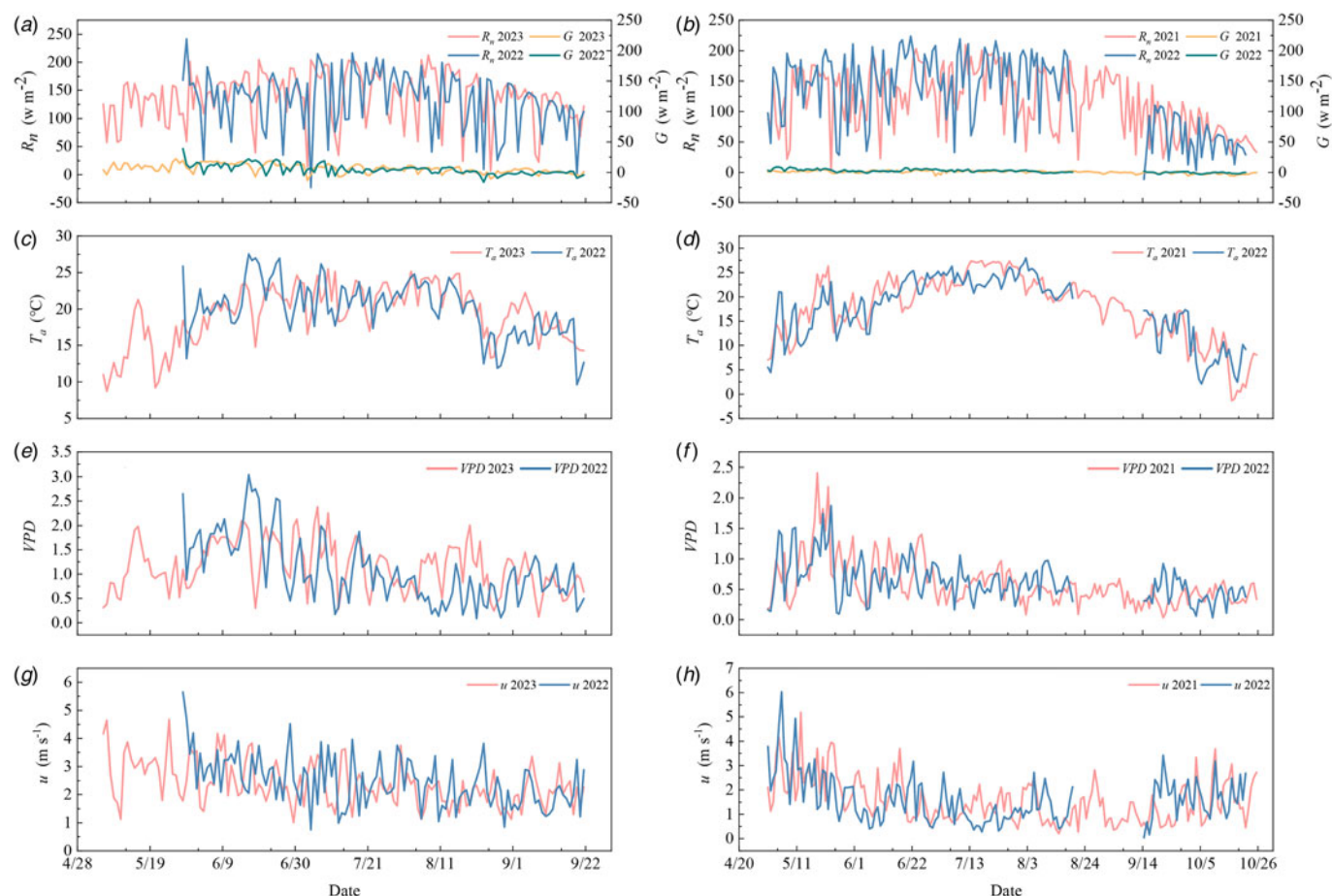


Figure 2. Variations of meteorological data during maize growing periods in two climatic regions.  $R_n$  is the net radiation,  $G$  is the soil heat flux,  $T_a$  is the air temperature,  $VPD$  is the vapour pressure deficit and  $u$  is the wind speed. (a), (c), (e) and (g) for northwestern China, (b), (d), (f) and (h) for northeastern China.

which ranges from 0 (worst fit) to 1 (perfect fit) (Yan *et al.*, 2019; Zhao *et al.*, 2023; Wang *et al.*, 2024a).

The optimal upscaling methods based on the four accuracy evaluation indexes differed at different fertility stages, but also the optimal upscaling moments were not exactly the same, and thus the global performance indicators (*GPI*) was introduced to comprehensively evaluate the optimal upscaling times of the four models (Despotovic *et al.*, 2015). The calculation formula is as follows:

$$GPI_i = \sum_{j=1}^4 \alpha_j (y_j - y_{ij}) \quad (16)$$

As for indicators of  $R^2$  and  $\varepsilon$ ,  $\alpha_j$  is equal to  $-1$ , while as for other indicators,  $\alpha_j$  is equal to  $1$ ,  $y_j$  is the median scale value of the index  $j$  and  $y_{ij}$  is the scale value of the index  $j$  in the model  $i$ . The higher the *GPI* value is, the higher the accuracy of the model is.

## Results

### Meteorological conditions

The observed meteorological data during the growing periods of maize in two climatic regions are shown in Fig. 2. For the NW station, the net radiation ( $R_n$ ) in 2022 (from 12 May to 26 Sep)

ranged from  $-22.8$  to  $241.6$   $W/m^2$ , with average value of  $132.0$   $W/m^2$ , and the corresponding values ranged from  $6.96$  to  $213.0$   $W/m^2$ , with average value of  $139.0$   $W/m^2$  in 2023 (from 6 May to 22 Sep). The soil heat flux ( $G$ ) in 2022 ranged from  $-16.2$  to  $39.1$   $W/m^2$ , with average value of  $4.33$   $W/m^2$ , and the corresponding value ranged from  $-13.5$  to  $22.2$   $W/m^2$ , with average value of  $6.23$   $W/m^2$  in 2023.

The air temperature ( $T_a$ ) in 2022 ranged from  $8.71$  to  $27.5$   $^{\circ}C$ , with average value equalled  $19.8$   $^{\circ}C$ , while  $T_a$  in 2023 ranged from  $8.75$  to  $25.5$   $^{\circ}C$ , with average value equalled  $19.2$   $^{\circ}C$ . The vapour pressure deficit (*VPD*) in 2022 ranged from  $0.09$  to  $3.04$   $kPa$ , with average value equalled  $1.06$   $kPa$ , while *VPD* in 2023 ranged from  $0.12$  to  $2.38$   $kPa$ , with average value equalled  $1.15$   $kPa$ . The wind speed ( $u$ ) had mean values of  $2.45$   $m/s$  for 2022 and  $2.38$   $m/s$  for 2023, with maximum values of  $5.65$  and  $4.68$   $m/s$ .

For the NE station, the  $R_n$  in 2021 (from 1 May to 26 Oct) ranged from  $3.27$  to  $209.7$   $W/m^2$ , with average value of  $116.3$   $W/m^2$  and the corresponding values ranged from  $-11.7$  to  $223.7$   $W/m^2$ , with average value of  $126.5$   $W/m^2$  in 2022 (from 1 May to 22 Oct). The  $G$  in 2021 ranged from  $-6.07$  to  $4.94$   $W/m^2$ , with average value of  $0.35$   $W/m^2$ , and the corresponding values ranged from  $-3.17$  to  $8.71$   $W/m^2$ , with average value of  $1.94$   $W/m^2$  in 2022. The  $T_a$  in 2021 ranged from  $-1.34$  to  $27.4$   $^{\circ}C$ , with average value equalled  $17.7$   $^{\circ}C$ , while  $T_a$  in 2022 ranged from  $2.12$  to  $28.0$   $^{\circ}C$ , with average value equalled  $17.7$   $^{\circ}C$ . The *VPD* in 2021 ranged from  $0.03$  to  $2.41$   $kPa$ , with average value equalled  $0.59$   $kPa$ ,

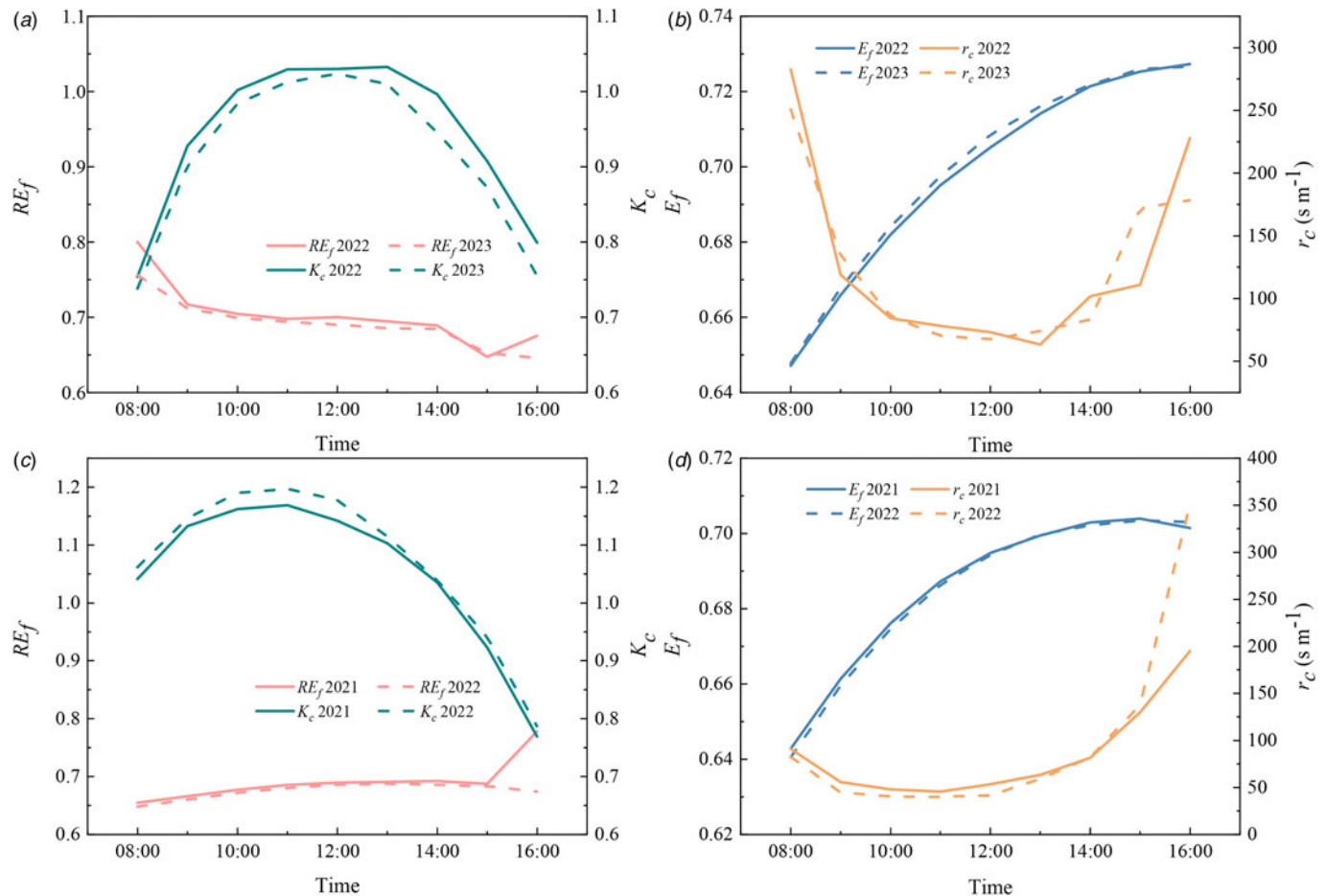


**Figure 3.** Hourly variations in calculated evaporative fraction ( $E_f$ ), revised evaporative fraction ( $RE_f$ ), crop coefficient ( $K_c$ ) and canopy resistance ( $r_c$ ) for maize. (a), (b) for northwestern China and (c), (d) for northeastern China.

while VPD in 2022 ranged from 0.03 to 1.88 kPa, with average value equalled 0.63 kPa. The  $u$  had mean values of 1.55 m/s for 2021 and 1.62 m/s for 2022, with maximum values of 5.18 and 6.03 m/s.

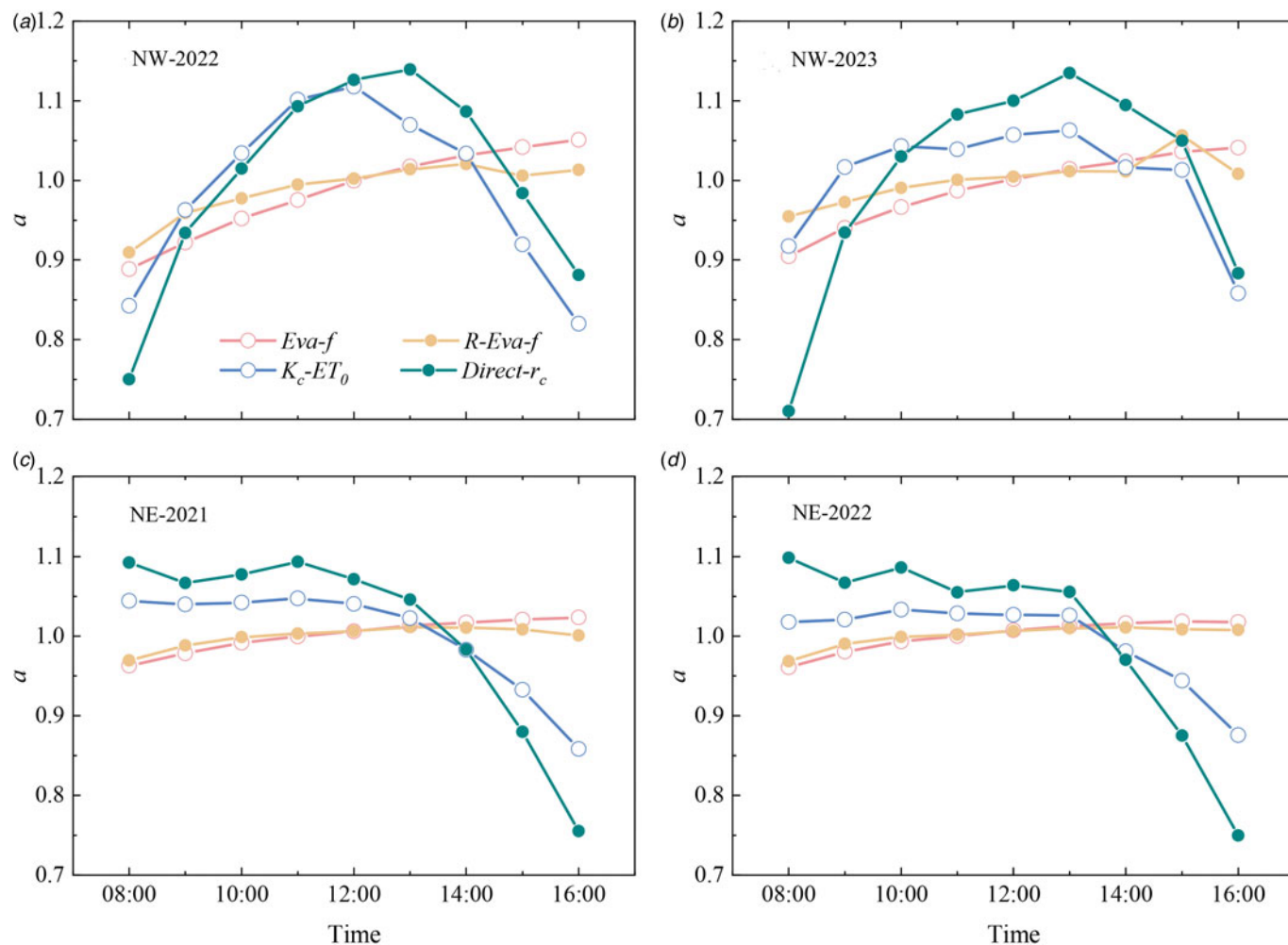
**Validity of the constancy of the upscaling factors**

Figure 3 is the diurnal variations of the evaporative fraction ( $E_f$ ), revised evaporative fraction ( $RE_f$ ), crop coefficient ( $K_c$ ), and canopy resistance ( $r_c$ ) obtained by averaging the parameters during 2022–2023 and 2021–2022 maize growing seasons in NW and NE, respectively. The amplitude of variations in the  $E_f$ ,  $RE_f$ ,  $K_c$  and  $r_c$  were similar over NW and NE. Specifically, the  $E_f$  showed a slightly increasing trend and ranged from 0.6 to 0.8 over both areas, which attributed the reason to the dry weather conditions (Hoedjes *et al.*, 2008; Yang *et al.*, 2013). The diurnal pattern of  $RE_f$  remained constant for most of the time except for the period close to sunrise and sunset, which may be due to lower available energy flux to drive  $ET$  in the early morning and the late afternoon (Yan *et al.*, 2022b).

The parameter  $K_c$  exhibited a typical down-concave shape throughout the day, with relatively sharp variations in the early morning and late afternoon, and reached a maximum near mid-day. The turbulent exchange was intense, especially after sunrise

and before sunset. The latent heat flux varied greatly, and the susceptibility of wind speed was obvious. The  $ET$  capacity and  $ET$  intensity of the subsurface were affected, so that  $K_c$  fluctuated greatly. However, the calculation of the  $E_f$  ignored these effects and assumed that the impedance was constant, and thus the fluctuation was small. The trend of  $K_c$  in this study was consistent with previous studies (Liu *et al.*, 2012a; Yan *et al.*, 2022b). However, the magnitude of  $K_c$  was usually higher than  $E_f$ , which was related to soil moisture stress and vegetation cover (Zhang *et al.*, 2017).

The trend of  $r_c$  exhibited a dramatically declining tendency in the early morning and late afternoon, while maintaining steady for the majority of the day, with a mean of 125 s/m in the NW, and 91 s/m in the NE. The rapid increase in  $r_c$  was partly due to the high atmospheric stability in the late afternoon, which reduced the soil water content and the overall resistance to evapotranspiration in the maize field. On the other hand, because the  $R_n$  decreased rapidly in the afternoon, but the decrease of  $G$  lagged behind that of  $R_n$ , so the calculated effective energy was smaller than that of the actual effective energy, and the inverse calculation of  $r_c$  using the P-M formula was on the large side, and the estimated  $\lambda ET_d$  was on the small side. The daily variations of  $E_f$  and  $K_c$  were mainly affected by stomatal regulation and the diurnal pattern of  $T_a$ , VPD and relative humidity, which has



**Figure 4.** Slopes ( $\alpha$ ) obtained by comparing the simulated daily evapotranspiration ( $\lambda ET_d$ ) of the four upscaling methods with the measured  $\lambda ET_d$  based on the Bowen ratio energy balance system (BREB) method. (a), (b) For northwestern China and (c), (d) for northeastern China.

strong effects on stomatal resistance (Yang *et al.*, 2013; Liu *et al.*, 2020).

### Performance of the four upscaling methods

Based on  $\lambda ET_d$  estimated by the *BREB* method, the efficacy of four upscaling methods (*Eva-f*, *R-Eva-f*,  $K_c-ET_0$  and *Direct-r<sub>c</sub>* methods) for estimating  $\lambda ET_d$  of NW and NE maize based on  $\lambda ET_i$  for the time period 08:00–16:00 was verified. The  $\lambda ET_i$  between 08:00 and 16:00 was chosen because it coincided with the time when the majority of satellites emerge over the study area and the upscaling factors are relatively stable.

The correlations between the estimated and measured  $\lambda ET_d$  at different hourly periods (08:00–16:00) for the four methods are shown in Figs 4 and 5. The slopes ( $\alpha$ ) of the fits of the four scaling methods at the two stations showed different degrees of intraday decreasing or increasing, which indicated that the four scaling methods had great variability in the calculation results for estimating  $\lambda ET_d$  using  $\lambda ET_i$  at different moments. The slopes of the measured and estimated  $\lambda ET_d$  by *Eva-f* and *R-Eva-f* methods for both climatic zones were the closest to 1 during the 10:00–14:00 time period, were the smallest during the 08:00–10:00 time period, were the largest during the 14:00–16:00 time period, and then increased, but the slopes did

not vary much from one time period to the next. The slopes of the  $K_c-ET_0$  and *Direct-r<sub>c</sub>* methods varied drastically, with different trends in magnitude. In 2022, the slopes in NW region increased and then decreased from 08:00 to 16:00, and were the closest to 1 for the time period 09:00–11:00 and 13:00–15:00, respectively. In 2023, the slopes in NW region increased from 08:00 to 16:00, and were the closest to 1 for the time period 09:00–11:00 and 13:00–15:00, respectively. The slopes in NW region showed an increase and then a gradual stabilization and then a decrease from 08:00 to 16:00, and was the closest to 1 in the 09:00–15:00 time period with similar variations in 2021 and 2022, and both showed gradual decrease, and a rapid decrease after 13:00 which upscales the estimated  $\lambda ET_d$  larger than the measured value. The coefficients of determination ( $R^2$ ) of the estimation results of the four methods were mostly located near 1, indicating a strong correlation between the measured and estimated  $\lambda ET_d$ . The simulation results of the four methods were the closest to each other during the 10:00–14:00 time period. In terms of the fitted  $R^2$ , all four methods showed high in midday and low in morning and afternoon. Previous studies found a minor divergence between measured  $\lambda ET_d$  and the estimations based on midday  $\lambda ET_i$  (Hoedjes *et al.*, 2008; Zhang *et al.*, 2017; Jiang *et al.*, 2021).

The mean absolute error (MAE) and relative root mean squared error (RRMSE) of the estimated  $\lambda ET_d$  calculated by

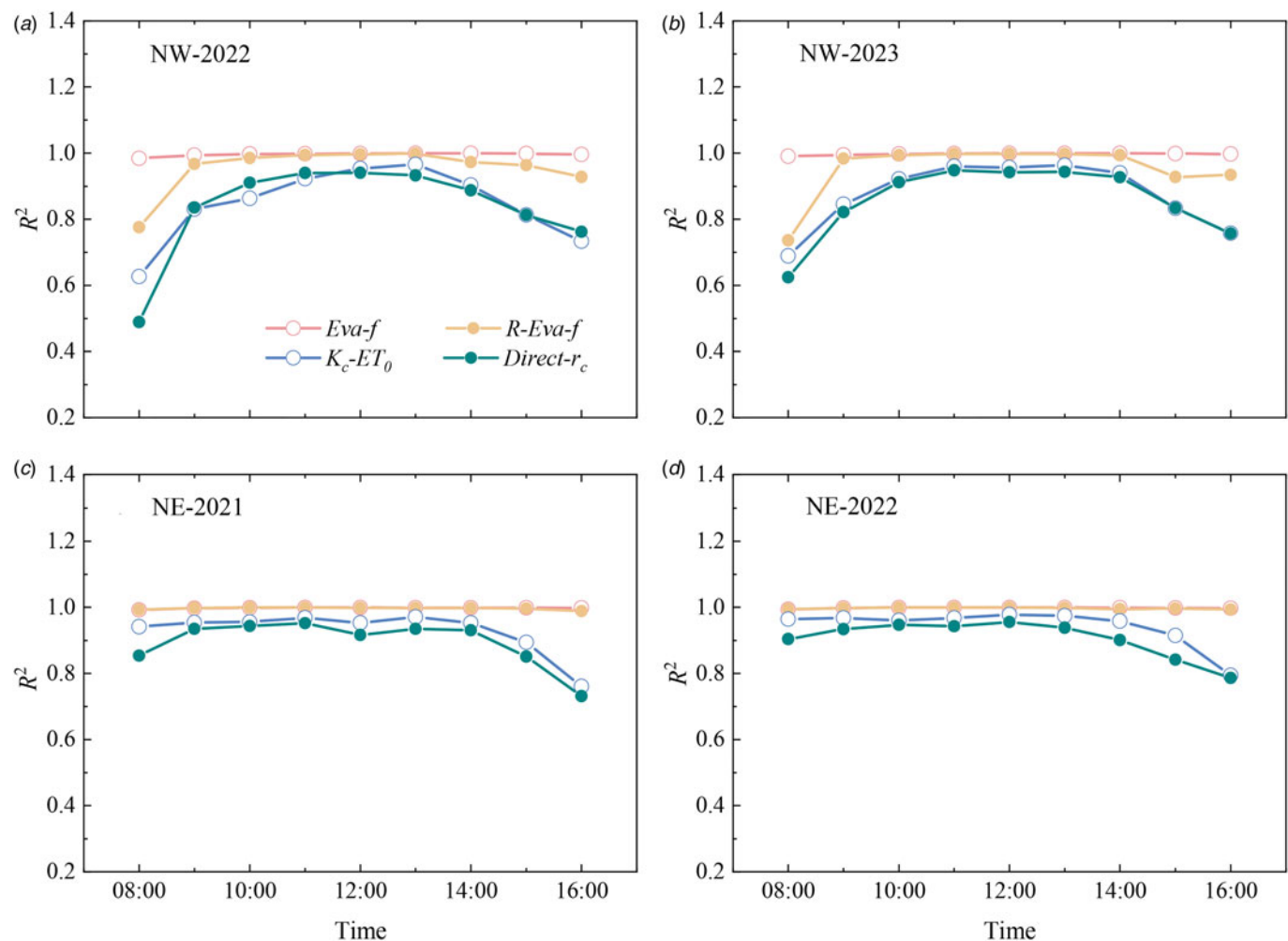


**Figure 5.** Coefficients of determination ( $R^2$ ) obtained by comparing the simulated daily evapotranspiration ( $\lambda ET_d$ ) of the four upscaling methods with the measured  $\lambda ET_d$  based on the Bowen ratio energy balance system (*BREB*) method. (a), (b) For northwestern China and (c), (d) for northeastern China.



four methods varied greatly as shown in Figs 6 and 7. The results of the MAE and RRMSE exhibited similar performance, with the *Eva-f* and *R-Eva-f* methods having the smallest MAE and RRMSE during the study periods. The  $K_c-ET_0$  and *Direct- $r_c$*  methods performed unstable, with a slightly higher MAE and RRMSE than the *Eva-f* and *R-Eva-f* methods. For the  $K_c-ET_0$  method, the MAE and RRMSE showed different performance for NW and NE, which the minimum values appeared when the  $\lambda ET_i$  was used at 14:00 and 13:00 for NW and NE, respectively. The results of MAE and RRMSE illustrated that the *Direct- $r_c$*  method exhibited similar performance in NW and NE. The trend of MAE and RRMSE showed upward concave shape, which confirmed the underperformance for most time in NW and NE. During the day, the MAE and RRMSE of the *Eva-f* and *R-Eva-f* methods were generally consistent, with average values of less than  $10.1 \text{ W/m}^2$  and 0.03. When using the  $\lambda ET_i$  from 9:00 to 15:00, the  $K_c-ET_0$  and *Direct- $r_c$*  methods had an average MAE of  $27.3 \text{ W/m}^2$ , which was considered satisfactory accuracy.

Moreover, diurnal variation of the efficiency coefficient ( $\varepsilon$ ) of four methods was displayed in Fig. 8. The hourly variations of  $\varepsilon$  for the *Eva-f* and *R-Eva-f* methods changed slightly and the values were more stable for NE than for NW. For the  $K_c-ET_0$  and *Direct- $r_c$*  methods, the trend of  $\varepsilon$  curves showed clear similarities.

For the NW station, the  $\varepsilon$  values of the  $K_c-ET_0$  and *Direct- $r_c$*  methods were lower when the  $\lambda ET_i$  in the morning was used, and remain around 0.6 for the rest of the day, but decreased obviously for the time period 10:00–14:00. For the NE station, the trend of  $\varepsilon$  curves sharply concaved down and attached the peak when the  $\lambda ET_i$  at 14:00 was used. Overall, the *Eva-f* method performed best and followed by the *R-Eva-f* method, with mean  $\varepsilon$  values less than 0.85 at all times; while the  $K_c-ET_0$  and *Direct- $r_c$*  methods performed worst in most cases. The mean  $\varepsilon$  values of the  $K_c-ET_0$  and *Direct- $r_c$*  method were only 0.55 and 0.46 for NW and 0.73 and 0.57 for NE, respectively.

From the above evaluation, it can be seen that not only the optimal upscaling methods based on the four accuracy evaluation indexes differed at different fertility stages, but also the optimal upscaling moments were not exactly the same, and thus the global performance indicators (*GPI*) was introduced to comprehensively evaluate the optimal upscaling times of the four models. Based on the four upscaling methods, the *GPI* of the calculated  $\lambda ET_d$  and measured values for different time intervals at the NW and NE stations were shown in Fig. 9. The larger the *GPI* value, the better the simulation performance. The four upscaling methods showed the ability to accurately simulate daily  $\lambda ET_d$  from 10:00 to 14:00, and the *Eva-f* and  $K_c-ET_0$  methods were superior to the  $K_c-ET_0$

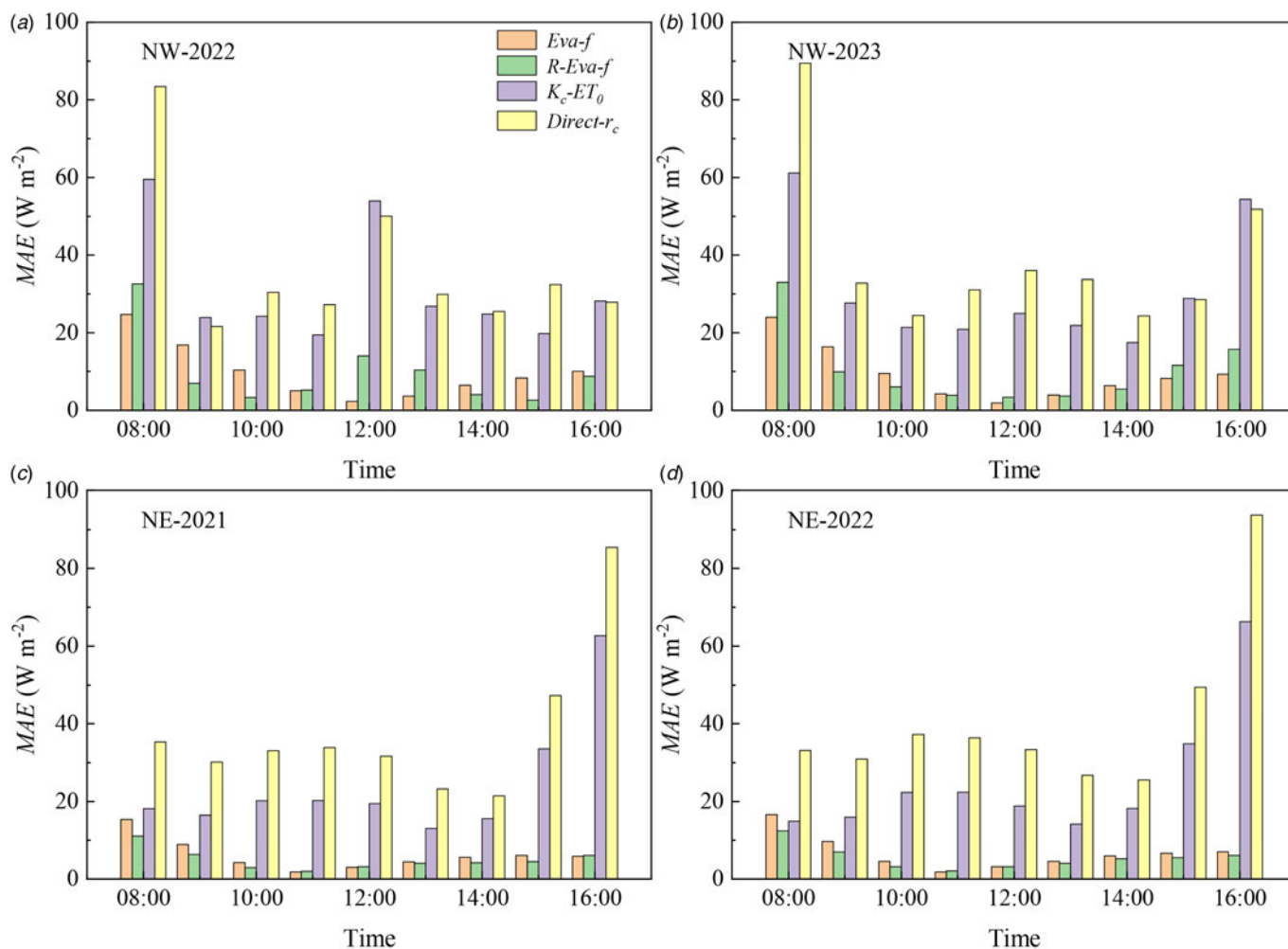


**Figure 6.** Mean absolute error (MAE) obtained by comparing the simulated daily evapotranspiration ( $\lambda ET_d$ ) of the four upscaling methods with the measured  $\lambda ET_d$  based on the Bowen ratio energy balance system (BREB) method. (a), (b) For northwestern China and (c), (d) for northeastern China.

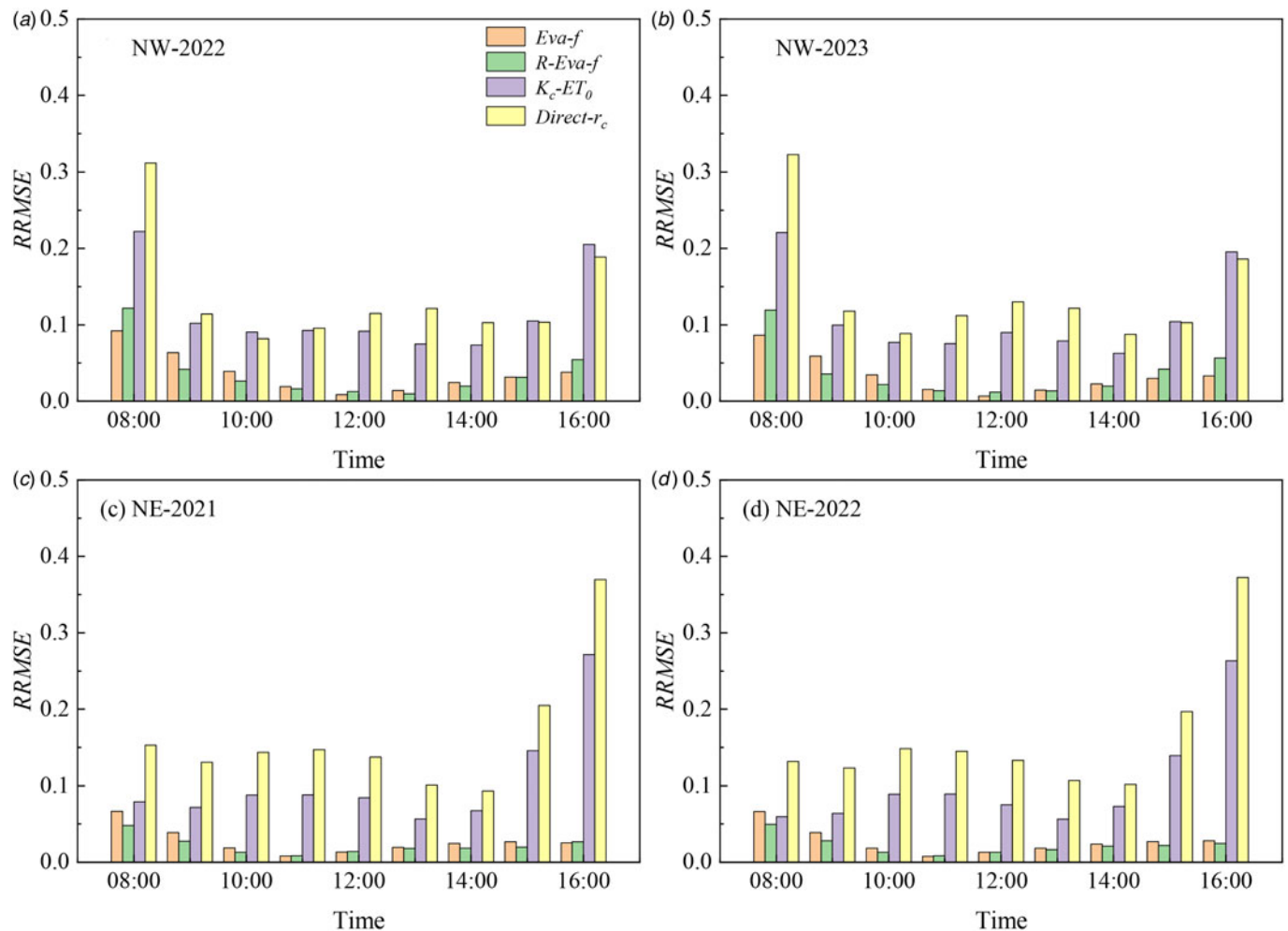


**Figure 7.** Relative root mean absolute error ( $RRMSE$ ) obtained by comparing the simulated daily evapotranspiration ( $\lambda ET_d$ ) of the four upscaling methods with the measured  $\lambda ET_d$  based on the Bowen ratio energy balance system ( $BREB$ ) method. (a), (b) For northwestern China and (c), (d) for northeastern China.

and  $Direct-r_c$  methods. However, the  $GPI$  of the four methods decreased obviously when the  $\lambda ET_i$  in the morning and afternoon was used. Overall, the  $Eva-f$  method performed best at 12:00 for the NW station, with the mean  $GPI$  of 0.55 for two years. At the NE station, the  $R-Eva-f$  method performed best at 14:00, with the mean  $GPI$  of 1.04 for two years.

## Discussion

The key parameters for upscaling methods ( $Eva-f$ ,  $R-Eva-f$ ,  $K_c-ET_0$  and  $Direct-r_c$  method) showed different characteristics of variation and temporal representativeness. The results of this study showed that the  $E_f$  and  $RE_f$  in the process of estimating  $\lambda ET_i$  to  $\lambda ET_d$  changed slightly through the day, which is similar to the results of Zhang et al. (2017) on maize in north China. However, Yan et al. (2022b) showed that the  $E_f$  and  $RE_f$  showed an arch shape for a tea and wheat field during the day in southeast China. This difference may be due to the difference in meteorological factors, leaf area index and crop physiological mechanisms. It may also be due to the fact that solar radiation was lower in the morning and afternoon, resulting in less available energy flux to drive  $ET$ . Thus, the results in the calculated  $E_f$  and  $RE_f$  were unstable in these time periods. The  $K_c$  displayed a somewhat concave-down

shape through the day, with comparatively sharp variations in the early morning and late afternoon. The  $K_c$  was not only related to the crop type, but also closely related to the climatic conditions, volumetric soil water content, crop cultivation conditions, irrigation and drainage management in the study areas. It is difficult to use the same set of  $K_c$  variation rules to reflect the  $\lambda ET_d$ , so it is necessary to determine the  $K_c$  based on the actual conditions of the study areas to accurately estimate the  $\lambda ET_d$  (Bezerra et al., 2012). The trend of  $r_c$  showed a typical concave-up shape through the day. Due to the problem of condensate re-evaporation after sunrise, the  $r_c$  values back-calculated with the P-M formula were too small or even less than 0, which was similar to the results of the previous study (Perez et al., 2005). The  $r_c$  values appeared to be constant with a slight increase in shape for the time period 12:00–14:00, which was attributed to an increase in  $r_c$  due to partial stomatal closure at midday when the light was stronger (Allen et al., 2006). The change of  $r_c$  were influenced by field climate, such as  $R_n$ ,  $VPD$ , etc. (Liu et al., 2020). The trend of  $r_c$  showed to sharply increase in the late afternoon. Specifically, on the one hand, crop stomatal conductance decreased with decrease in radiation intensity, so  $r_c$  increased rapidly near noon. In most cases, all four upscaling methods showed some degree of underestimation, with better performance during the middle of the day

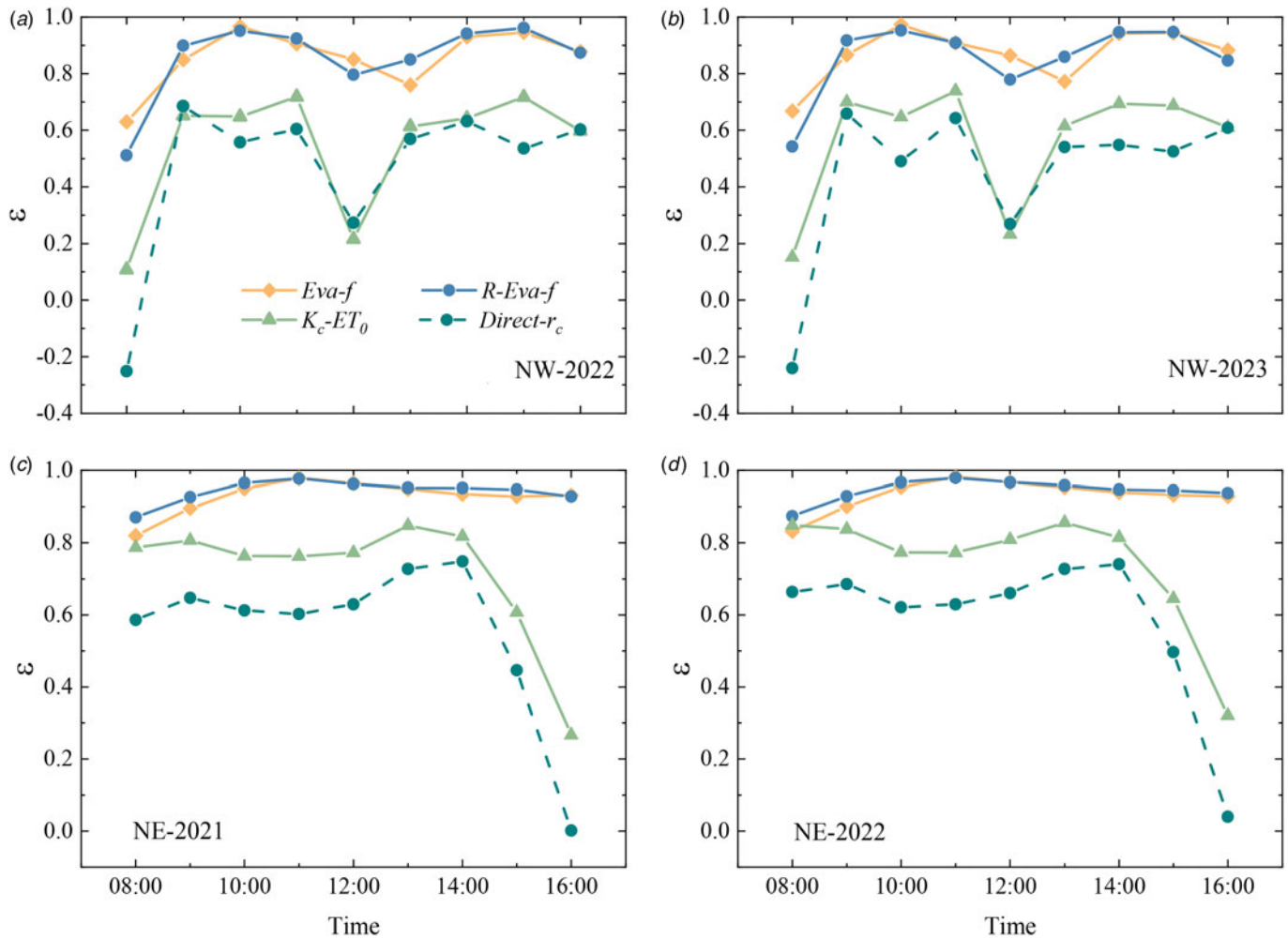


**Figure 8.** Coefficient of efficiency ( $\epsilon$ ) obtained by comparing the simulated daily evapotranspiration ( $\lambda ET_d$ ) of the four upscaling methods with the measured  $\lambda ET_d$  based on the Bowen ratio energy balance system (BREB) method. (a), (b) For northwestern China and (c), (d) for northeastern China.

than in the morning and afternoon, which agreed with other research results (Tang and Li, 2017; Zhang *et al.*, 2017). The presence of clouds and energy conditions may be a potential reason for the underestimation of  $\lambda ET_d$  (Delogu *et al.*, 2012; Tang *et al.*, 2017; Jiang *et al.*, 2018).

In this study, we found that the *Eva-f* method performed best for the time period 11:00–2:00 in both NW and NE stations. The *R-Eva-f* method performed best for the time period 10:00–11:00 for the NW station and for the time period 10:00–12:00 for the NE station. Yan *et al.* (2022b) and Liu (2021) concluded that the optimal upscaling time period of the *Eva-f* and *R-Eva-f* methods was from 09:00 to 15:00, particularly for instantaneous values between 11:00 and 14:00. In addition, Zhang *et al.* (2017) showed that the optimal upscaling moment of the *Eva-f* method was 14:00–15:00 on maize. The reason for this difference was mainly due to the difference in the geographical location of the study regions. The difference in sunrise and sunset times in different geographical locations led to the slight difference in optimal upscaling moment of the study regions. Liu *et al.* (2011) found that the  $K_c$  remained mostly constant during the reproductive period of wheat. The values in the morning (10:00–11:00) and afternoon (14:00–15:00) were the most similar to the daily average values, which were less than 1. Chávez *et al.* (2008) and

Katimbo *et al.* (2022) found that the accuracy of estimating  $\lambda ET_d$  using the  $K_c-ET_0$  method was not as good as the *Eva-f* method, but the accuracy of the estimation could be improved by using the  $K_c$  values during the midday. There was a clear intra-day variation characteristic of  $K_c$  in this study. At the NW station, the fluctuation of  $K_c$  was smaller from 10:00 to 14:00. The fluctuation of  $K_c$  was smaller from 10:00 to 12:00 for the NE station. Thus, it was seen that the study of the optimal upscaling timing in different regions was an important prerequisite for the improvement of the estimation accuracy of  $\lambda ET_d$  by the  $K_c-ET_0$  method. From the analysis of  $r_c$ , it was concluded that the  $r_c$  values for the time period 10:00–11:00 instead of daily average value were more effective in estimating  $\lambda ET_d$  for the NW station. At the NE station, the  $r_c$  for the time period 13:00–14:00 instead of daily value were more effective in estimating  $\lambda ET_d$ . This period coincided with the time of remote sensing satellite transit, and the time period (9:00–11:00) is the process of atmospheric stability changing from stable to unstable, which is in line with the condition of atmospheric neutral stability assumed by aerodynamic drag.

Taken together, both the *Eva-f* and *R-Eva-f* methods achieved good results in modelling  $\lambda ET_d$  from  $\lambda ET_i$  at most of the time. However, the *R-Eva-f* method was slightly inferior to the *Eva-f* method for two different climatic regions, and similar conclusions

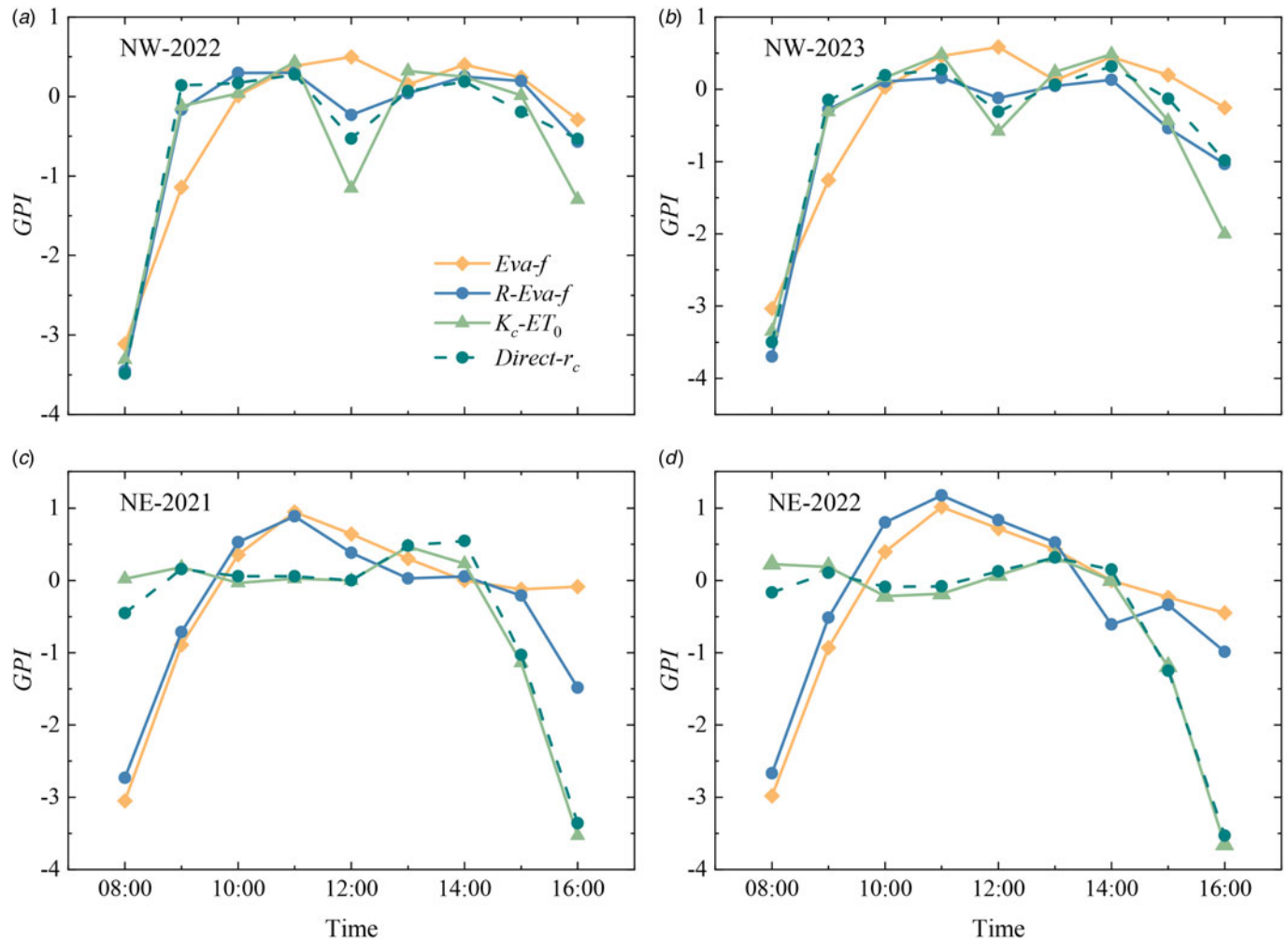


**Figure 9.** Global performance indicators (GPI) of four upscaling methods at different times. (a), (b) For northwestern China and (c), (d) for northeastern China.

were obtained by Yan *et al.* (2022b) for tea and wheat in southeast China. Liu (2021) reported the *Eva-f* method, which uses potential evapotranspiration and incoming shortwave radiation, outperformed the other methods for simulating daily series. Chen *et al.* (2013) and Jiang *et al.* (2021) concluded that the *R-Eva-f* method performed best for most ecosystems. This discrepancy was mainly due to errors in the observation of  $G$ , where the soil heat flux sensors were buried in the soil surface and were affected by changes in wind speed, soil properties and soil moisture. However, Cammalleri *et al.* (2014) pointed out that if the daily fluxes were for 24 h instead of just the daytime, the influence of  $G$  might not be as significant. Yang *et al.* (2013) showed that the diurnal pattern of  $K_c$  was strongly dependent on the leaf area index (LAI) and the  $K_c-ET_0$  method may perform poorly at higher LAI, whereas Zhang *et al.* (2017) reported the performance of the  $K_c-ET_0$  methods was good under various LAI. The *Direct-rc* method showed poor estimation results in most intervals, which suggested the *Direct-rc* method in extrapolating  $\lambda ET_i$  into  $\lambda ET_d$  may not be valid in this study and is no longer robust and universally applicable.

## Conclusion

In this study, we evaluated four upscaling methods (*Eva-f*, *R-Eva-f*,  $K_c-ET_0$  and *Direct-rc* methods) performance in

estimating  $\lambda ET_d$  from  $\lambda ET_i$ , using the measurements of  $\lambda ET_d$  by Bowen ratio energy balance system in two different climatic regions of Northwest and Northeast China based on the measured data from 2021 to 2023, and the following conclusions were drawn:

- (1) The key parameters  $E_f$ ,  $RE_f$ ,  $K_c$  and  $r_c$  of  $\lambda ET_i$  to  $\lambda ET_d$  upscaling had obvious daily variation characteristics, and the overall trends were consistent in the two regions, with  $E_f$  and  $RE_f$  behaving more closely than  $K_c$  and  $r_c$ .
- (2) The *Eva-f* and *R-Eva-f* methods were better than the other two methods ( $K_c-ET_0$  and *Direct-rc* methods) in all evaluation indexes, but the *R-Eva-f* method was slightly inferior to the *Eva-f* method due to the neglect of soil heat flux ( $G$ ). Both the *Eva-f* and *R-Eva-f* methods were more suitable for the Northwest and Northeast regions.
- (3) The time for  $\lambda ET_i$  had a significant effect on estimating  $\lambda ET_d$  by upscaling methods. Specifically, at the NW station, the *Eva-f* method gave the best scaling when  $\lambda ET_i$  at 12:00 was used, while at the NE station, the  $\lambda ET_d$  simulation had the highest accuracy using the *R-Eva-f* method when the  $\lambda ET_i$  at 11:00 was used.
- (4) Therefore, it is recommended that the *Eva-f* method is the preferred method for upscaling evapotranspiration in the



Northwest region, with the moment of 12:00 being the optimal upscaling time. The *R-Eva-f* method is the best upscaling method for the Northeast region, with 11:00 being the optimal upscaling time.

**Author contributions.** Xuanxuan Wang, Biyu Wang, Haofang Yan, Chuan Zhang, Hexiang Zheng, Guoqing Wang, Jianyun Zhang and Bin He conceived and designed the study. Rongxuan Bao, Run Xue, Yudong Zhou, Jun Li, Rui Zhou, Beibei Hao and Yujing Han conducted data gathering. Xuanxuan Wang, Biyu Wang performed statistical analyses. Xuanxuan Wang, Biyu Wang and Haofang Yan wrote the article.

**Funding statement.** This study was financially supported by the National Key R&D Program (2021YFC3201103, 2023YFC3205701), the Natural Science Foundation of China (52121006, U2243228, 1509107, 42177065).

**Competing interests.** The authors declare that there is no conflict of interest, nor is there any commercial or competing interest, which is defined as a conflict of interest in connection with the work submitted.

**Ethical standards.** Not applicable.

## References

- Allen RG, Pruitt WO, Wright JL, Howell TA, Ventura F, Snyder R, Itenfisu D, Steduto P, Berengena J, Yrisarry JB, Smith M, Pereira LS, Raes D, Perrier A, Alves I, Walter I and Elliott R (2006) A recommendation on standardized surface resistance for hourly calculation of reference ET<sub>o</sub> by the FAO56 Penman–Monteith method. *Agricultural Water Management* **81**, 1–22.
- Allen RG, Tasumi M, Morse A, Trezza R, Wright JL, Bastiaanssen W, Kramber W, Lorite I and Robison CW (2007) Satellite-based energy balance for mapping evapotranspiration with internalized calibration (METRIC) – applications. *Journal of Irrigation and Drainage Engineering* **133**, 395–406.
- Bezerra BG, da Silva BB, Bezerra JRC, Sofiatti V and dos Santos CAC (2012) Evapotranspiration and crop coefficient for sprinkler-irrigated cotton crop in Apodi Plateau semiarid lands of Brazil. *Agricultural Water Management* **107**, 86–93.
- Cammalleri C, Anderson MC and Kustas WP (2014) Upscaling of evapotranspiration fluxes from instantaneous to daytime scales for thermal remote sensing applications. *Hydrology and Earth System Sciences* **18**, 1885–1894.
- Chávez JL, Neale CMU, Prueger JH and Kustas WP (2008) Daily evapotranspiration estimates from extrapolating instantaneous airborne remote sensing ET values. *Irrigation Science* **27**, 67–81.
- Chemin Y and Alexandridis T (2001) Improving spatial resolution of ET seasonal for irrigated rice in Zhanghe. *The 22nd Asian Conference on Remote Sensing* **5**, 9.
- Chen H, Yang D and Lü H (2013) Comparison of temporal extrapolation methods for evapotranspiration over variant underlying croplands. *Transactions of the Chinese Society of Agricultural Engineering* **29**, 73–81.
- Choudhury BU, Singh AK and Pradhan S (2013) Estimation of crop coefficients of dry-seeded irrigated rice-wheat rotation on raised beds by field water balance method in the Indo-Gangetic plains, India. *Agricultural Water Management* **123**, 20–31.
- Colaizzi PD, Evett SR, Howell TA and Tolk JA (2006) Comparison of five models to scale daily evapotranspiration from one-time-of-day measurements. *Transactions of the ASABE* **49**, 1409–1417.
- Delogu E, Boulet G, Olioso A, Couderc B, Chirouze J, Ceschia E, Le Dantec V, Marloie O, Chehbouni G and Lagouarde JP (2012) Reconstruction of temporal variations of evapotranspiration using instantaneous estimates at the time of satellite overpass. *Hydrology and Earth System Sciences* **16**, 2995–3010.
- Despotovic M, Nedic V, Despotovic D and Cvetanovic S (2015) Review and statistical analysis of different global solar radiation sunshine models. *Renewable and Sustainable Energy Reviews* **52**, 1869–1880.
- Disasa KN, Yan H, Wang G, Zhang J, Zhang C and Zhu X (2024) Projection of future precipitation, air temperature, and solar radiation changes in southeastern China. *Theoretical and Applied Climatology* **155**, 4481–4560.
- Evett SR, Schwartz RC, Howell TA, Louis Baumhardt R and Copeland KS (2012) Can weighing lysimeter ET represent surrounding field ET well enough to test flux station measurements of daily and sub-daily ET? *Advances in Water Resources* **50**, 79–90.
- Farah HO, Bastiaanssen WGM and Feddes RA (2004) Evaluation of the temporal variability of the evaporative fraction in a tropical watershed. *International Journal of Applied Earth Observation and Geoinformation* **5**, 129–140.
- Gao X, Mei X, Gu F, Hao W, Gong D and Li H (2018) Evapotranspiration partitioning and energy budget in a rainfed spring maize field on the Loess Plateau, China. *Catena* **166**, 249–259.
- Gentine P, Entekhabi D, Chehbouni A, Boulet G and Duchemin B (2007) Analysis of evaporative fraction diurnal behaviour. *Agricultural and Forest Meteorology* **143**, 13–29.
- Heilman JL and Brittin CL (1989) Fetch requirements for Bowen ratio measurements of latent and sensible heat fluxes. *Agricultural and Forest Meteorology* **44**, 261–273.
- Hoedjes JCB, Chehbouni A, Jacob F, Ezzahar J and Boulet G (2008) Deriving daily evapotranspiration from remotely sensed instantaneous evaporative fraction over olive orchard in semi-arid Morocco. *Journal of Hydrology* **354**, 53–64.
- Hossen MS, Mano M, Miyata A, Baten MA and Hiyama T (2011) Surface energy partitioning and evapotranspiration over a double-cropping paddy field in Bangladesh. *Hydrological Processes* **26**, 1311–1320.
- Jiang X, Kang S, Tong L, Li F, Li D, Ding R and Qiu R (2014) Crop coefficient and evapotranspiration of grain maize modified by planting density in an arid region of northwest China. *Agricultural Water Management* **142**, 135–143.
- Jiang Y, Tang R, Jiang X and Li Z-L (2018) Impact of clouds on the estimation of daily evapotranspiration from MODIS-derived instantaneous evapotranspiration using the constant global shortwave radiation ratio method. *International Journal of Remote Sensing* **40**, 1930–1944.
- Jiang L, Zhang B, Han S, Chen H and Wei Z (2021) Upscaling evapotranspiration from the instantaneous to the daily time scale: assessing six methods including an optimized coefficient based on worldwide eddy covariance flux network. *Journal of Hydrology* **596**, 126135.
- Jiang J, Yan H, Zhang C, Wang G, Zhang J, Liang S and Deng S (2024) Simulation of greenhouse cucumber evapotranspiration based on canopy-air temperature difference. *Journal of Drainage and Irrigation Machinery Engineering* **42**, 532–540.
- Jung M, Reichstein M, Ciais P, Seneviratne SI, Sheffield J, Goulden ML, Bonan G, Cescatti A, Chen J, de Jeu R, Dolman AJ, Eugster W, Gerten D, Gianelle D, Gobron N, Heinke J, Kimball J, Law BE, Montagnani L, Mu Q, Mueller B, Oleson K, Papale D, Richardson AD, Rouspard O, Running S, Tomelleri E, Viovy N, Weber U, Williams C, Wood E, Zaehle S and Zhang K (2010) Recent decline in the global land evapotranspiration trend due to limited moisture supply. *Nature* **467**, 951–954.
- Katimbo A, Rudnick DR, Liang W-Z, DeJonge KC, Lo TH, Franz TE, Ge Y, Qiao X, Kabenge I and Nakabuye HN (2022) Two source energy balance maize evapotranspiration estimates using close-canopy mobile infrared sensors and upscaling methods under variable water stress conditions. *Agricultural Water Management* **274**, 107972.
- Lakhiar IA, Yan H, Zhang J, Wang G, Deng S, Bao R, Zhang C, Syed TN, Wang B and Zhou R (2024) Plastic pollution in agriculture as a threat to food security, the ecosystem, and the environment: an overview. *Agronomy* **14**, 548.
- Li S, Kang S, Li F, Zhang L and Zhang B (2008) Vineyard evaporative fraction based on eddy covariance in an arid desert region of Northwest China. *Agricultural Water Management* **95**, 937–948.
- Li M, Yan H, Zhang C, Zhang J, Wang G and Acquah SJ (2024) Current deficiencies and needed enhancements on greenhouse crop evapotranspiration models. *Journal of Drainage and Irrigation Machinery Engineering* **42**, 57–63.
- Liu Z (2021) The accuracy of temporal upscaling of instantaneous evapotranspiration to daily values with seven upscaling methods. *Hydrology and Earth System Sciences* **25**, 4417–4433.

- Liu G, Liu Y and Xu D (2011) Investigation on performance of evapotranspiration temporal upscaling methods based on eddy covariance measurements. *Transactions of the Chinese Society of Agricultural Engineering* 27, 7–12.
- Liu G, Hafeez M, Liu Y, Xu D and Vote C (2012a) A novel method to convert daytime evapotranspiration into daily evapotranspiration based on variable canopy resistance. *Journal of Hydrology* 414–415, 278–283.
- Liu G, Liu Y, Hafeez M, Xu D and Vote C (2012b) Comparison of two methods to derive time series of actual evapotranspiration using eddy covariance measurements in the southeastern Australia. *Journal of Hydrology* 454–455, 1–6.
- Liu X, Yang S, Xu J, Zhang J and Liu J (2017) Effects of soil heat storage and phase shift correction on energy balance closure of paddy fields. *Atmosfera* 30, 39–52.
- Liu X, Xu J, Zhou X, Wang W and Yang S (2020) Evaporative fraction and its application in estimating daily evapotranspiration of water-saving irrigated rice field. *Journal of Hydrology* 584, 124317.
- Liu Y, Jiang Q, Wang Q, Jin Y, Yue Q, Yu J, Zheng Y, Jiang W and Yao X (2022) The divergence between potential and actual evapotranspiration: an insight from climate, water, and vegetation change. *Science of the Total Environment* 807, 150648.
- Ma Z, Yan N, Wu B, Stein A, Zhu W and Zeng H (2019) Variation in actual evapotranspiration following changes in climate and vegetation cover during an ecological restoration period (2000–2015) in the Loess Plateau, China. *Science of the Total Environment* 689, 534–545.
- Ma Z, Wu B, Yan N, Zhu W and Xu J (2021) Coupling water and carbon processes to estimate field-scale maize evapotranspiration with Sentinel-2 data. *Agricultural and Forest Meteorology* 306, 108421.
- Malek E, Bingham GE and Mccurdy GD (1992) Continuous measurement of aerodynamic and alfalfa canopy resistances using the Bowen ratio-energy balance and Penman–Monteith methods. *Boundary-Layer Meteorology* 59, 187–194.
- Miralles DG, De Jeu RAM, Gash JH, Holmes TRH and Dolman AJ (2011) Magnitude and variability of land evaporation and its components at the global scale. *Hydrology and Earth System Sciences* 15, 967–981.
- Mu Q, Zhao M and Running SW (2011) Improvements to a MODIS global terrestrial evapotranspiration algorithm. *Remote Sensing of Environment* 115, 1781–1800.
- Ohmura A (1982) Objective criteria for rejecting data for Bowen ratio flux calculations. *Journal of Applied Meteorology* 21, 595–598.
- Perez PJ, Lecina S, Castellvi F, Martínez-Cob A and Villalobos FJ (2005) A simple parameterization of bulk canopy resistance from climatic variables for estimating hourly evapotranspiration. *Hydrological Processes* 20, 515–532.
- Pozníková G, Fischer M, van Kesteren B, Orság M, Hlavinka P, Žalud Z and Trnka M (2018) Quantifying turbulent energy fluxes and evapotranspiration in agricultural field conditions: a comparison of micrometeorological methods. *Agricultural Water Management* 209, 249–263.
- Shuttleworth W, Gurney R, Hsu A and Ormsby J (1989) FIFE: the variation in energy partition at surface flux sites. *IAHS Publication* 186, 523–534.
- Sugita M and Brutsaert W (1991) Daily evaporation over a region from lower boundary layer profiles measured with radiosondes. *Water Resources Research* 27, 747–752.
- Suleiman A and Crago R (2004) Hourly and daytime evapotranspiration from grassland using radiometric surface temperatures. *Agronomy Journal* 96, 384–390.
- Tang R and Li ZL (2017) An improved constant evaporative fraction method for estimating daily evapotranspiration from remotely sensed instantaneous observations. *Geophysical Research Letters* 44, 2319–2326.
- Tang R, Li Z-L and Sun X (2013) Temporal upscaling of instantaneous evapotranspiration: an intercomparison of four methods using eddy covariance measurements and MODIS data. *Remote Sensing of Environment* 138, 102–118.
- Tang R, Li ZL, Sun X and Bi Y (2017) Temporal upscaling of instantaneous evapotranspiration on clear-sky days using the constant reference evaporative fraction method with fixed or variable surface resistances at two cropland sites. *Journal of Geophysical Research: Atmospheres* 122, 784–801.
- Thom A (1972) Momentum, mass and heat exchange of vegetation. *Journal of the Royal Meteorological Society* 98, 124–134.
- Van Niel TG, McVicar TR, Roderick ML, van Dijk AIJM, Renzullo LJ and van Gorsel E (2011) Correcting for systematic error in satellite-derived latent heat flux due to assumptions in temporal scaling: assessment from flux tower observations. *Journal of Hydrology* 409, 140–148.
- Van Niel TG, McVicar TR, Roderick ML, van Dijk AIJM, Beringer J, Hutley LB and van Gorsel E (2012) Upscaling latent heat flux for thermal remote sensing studies: comparison of alternative approaches and correction of bias. *Journal of Hydrology* 468–469, 35–46.
- Wandera L, Mallick K, Kiely G, Rouspard O, Pechl M and Magliulo V (2017) Upscaling instantaneous to daily evapotranspiration using modelled daily shortwave radiation for remote sensing applications: an artificial neural network approach. *Hydrology and Earth System Sciences* 21, 197–215.
- Wang B, Bao R, Yan H, Zheng H, Wu J, Zhang C and Wang G (2024a) Study of evapotranspiration and crop coefficients for eggplant in a Venlo-type greenhouse in South China. *Irrigation and Drainage*.
- Wang B, Yan H, Zheng H, Wu J, Tian D, Zhang C, Zhu X, Wang G, Lakhari IA and Liu Y (2024b) Estimation of latent heat flux of pasture and maize in arid region of Northwest China based on canopy resistance modeling. *Frontiers in Environmental Science* 12, 1397704.
- Xu T, Liu S, Xu L, Chen Y, Jia Z, Xu Z and Nielson J (2015) Temporal upscaling and reconstruction of thermal remotely sensed instantaneous evapotranspiration. *Remote Sensing* 7, 3400–3425.
- Xu X, Li X, Wang X, He C, Tian W, Tian J and Yang L (2020) Estimating daily evapotranspiration in the agricultural-pastoral ecotone in Northwest China: a comparative analysis of the complementary relationship, WRF-CLM4.0, and WRF-Noah methods. *Science of the Total Environment* 729, 138635.
- Yan H, Zhang C, Coenders Gerrits M, Acquah SJ, Zhang H, Wu H, Zhao B, Huang S and Fu H (2018) Parametrization of aerodynamic and canopy resistances for modeling evapotranspiration of greenhouse cucumber. *Agricultural and Forest Meteorology* 262, 370–378.
- Yan H, Acquah SJ, Zhang C, Wang G, Huang S, Zhang H, Zhao B and Wu H (2019) Energy partitioning of greenhouse cucumber based on the application of Penman-Monteith and bulk transfer models. *Agricultural Water Management* 217, 201–211.
- Yan H, Yu J, Zhang C, Wang G, Huang S and Ma J (2021) Comparison of two canopy resistance models to estimate evapotranspiration for tea and wheat in southeast China. *Agricultural Water Management* 245, 106581.
- Yan H, Huang S, Zhang J, Zhang C, Wang G, Li L, Zhao S, Li M and Zhao B (2022a) Comparison of Shuttleworth–Wallace and dual crop coefficient method for estimating evapotranspiration of a tea field in Southeast China. *Agriculture* 12, 1392.
- Yan H, Li M, Zhang C, Zhang J, Wang G, Yu J, Ma J and Zhao S (2022b) Comparison of evapotranspiration upscaling methods from instantaneous to daytime scale for tea and wheat in southeast China. *Agricultural Water Management* 264, 107464.
- Yan H, Deng S, Zhang C, Wang G, Zhao S, Li M, Liang S, Jiang J and Zhou Y (2023) Determination of energy partition of a cucumber grown venlo-type greenhouse in southeast China. *Agricultural Water Management* 276, 108047.
- Yang D-W, Chen H and Lei H-M (2013) Analysis of the diurnal pattern of evaporative fraction and its controlling factors over croplands in the Northern China. *Journal of Integrative Agriculture* 12, 1316–1329.
- Yang P, Hu H, Tian F, Zhang Z and Dai C (2016) Crop coefficient for cotton under plastic mulch and drip irrigation based on eddy covariance observation in an arid area of northwestern China. *Agricultural Water Management* 171, 21–30.
- Zhang BZ, Kang SZ, Zhang L, Du TS, Li SE and Yang XY (2010) Estimation of seasonal crop water consumption in a vineyard using Bowen ratio-energy balance method. *Hydrological Processes* 21, 3635–3641.
- Zhang B, Chen H, Xu D and Li F (2017) Methods to estimate daily evapotranspiration from hourly evapotranspiration. *Biosystems Engineering* 153, 129–139.
- Zhang Y, Kong D, Gan R, Chiew FHS, McVicar TR, Zhang Q and Yang Y (2019) Coupled estimation of 500 m and 8-day resolution global evapotranspiration and gross primary production in 2002–2017. *Remote Sensing of Environment* 222, 165–182.
- Zhao S, Yan H, Zhang C, Li M, Deng S, Liang S and Jiang J (2023) Estimation of cucumber evapotranspiration in greenhouse based on improved dual crop coefficient model and Priestley-Taylor model. *Journal of Drainage and Irrigation Machinery Engineering* 41, 849–857.